OTHER PROBLEMS
OF PHYSICAL CHEMISTRY

A Second-Order Saddle Point in the Reaction Coordinate for the Isomerization of the NH_5 Complex: Ab initio Calculations

R. M. Minyaev[1], I. V. Getmanskii[1], and W. Quapp[2]

[1]*Research Institute of Physical and Organic Chemistry, Rostov State University, Rostov-on-Don, Russia*
[2]*Institute of Mathematics, Leipzig University, Germany*
E-mail: minyaev@ipoc.rsu.ru
Received August 5, 2003

Abstract—The existence of a second-order saddle point in the reaction coordinate for the decomposition of the D_{3h}-symmetry NH_5 system, the point that corresponds to a first-order saddle point (the true transition state), was predicted by CCD(full)/6-311++G($3df$, $2p$) calculations. The potential energy surface was found to exhibit an unusual topology in the vicinity of the second-order saddle point. It was established that the $NH_3\cdots H_2$ bimolecular complex corresponds to a minimum in the potential energy surface with a very low energy of complexation (~0.02 kcal/mol).

Molecular interactions play an important role in the formation of various gas-phase complexes and clusters and determine the secondary and tertiary structures of biologically important molecules and the molecular packing of crystals [1–7]. One of the most important types of molecular interactions is the donor–acceptor interaction of main-group elements [2–4, 6]. In the last twenty years, donor–acceptor complexes in the gas phase have been receiving ever increasing attention [3–7]. Theoretical and experimental studies of Van der Waals, electrostatic, and donor–acceptor complexes in the gas phase have provided better insights into the nature of the specific attractive forces acting between electron-deficient and electron-abundant centers in molecules.

The aim of this work was to perform an ab initio study of the interaction between the H_2 and NH_3 molecules in the gas phase, the formation of weakly bonded complexes **I** and **II**, and the influence of weak interaction on the pyramidal inversion of the ammonia molecule in the complex (**I** ⇌ **III** ⇌ **II**):

(**I**), C_{3v} (**III**), C_{3v} (TS) (**II**), C_{3v}
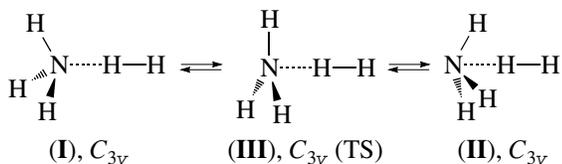
Apart from the structural characteristics of the $NH_3\cdots H_2$ donor–acceptor interaction, particular attention was given to the topology of the potential energy surface (PES) of the NH_5 system in the vicinity of the structures

(**IV**), D_{3h} (TS)   (**V**), C_{3v} (Hill Top)   (**VI**), C_{2v} (TS)
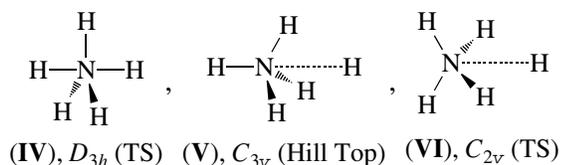
and to the unusual reaction coordinates of the rearrangements of these structures.

Despite many debatable examples [8–4], the reaction coordinate is considered to be a smooth continuous line connecting the saddle point (the transition state) with the two minimums corresponding to the reactant and the product [15]. It has been shown [8, 9, 12] that a line of steepest descent (gradient line) can connect two neighboring saddle points. In this case, the reaction coordinate may consist of several orthogonal gradient lines intersecting one another at the saddle point [9]. In this work, we considered the first example of a reaction coordinate (line of steepest descent) coming out from saddle point **IV** ($\lambda = 1$; thereafter, λ is the number of negative Hessian eigenvalues) along the direction tangential to the transition vector and coming to neighboring stationary point **V**, which is a second-order saddle point (the top of a two-dimensional hill; $\lambda = 2$) [16].

CALCULATION PROCEDURE

The positions and characteristics of the stationary points were calculated by the standard method of coupled cluster doublets, CCD(full)/6-311++G($3df$, $2p$), using the Gaussian 98 package [17]. The molecular geometry at the stationary points was optimized using the tight convergence criterion at all approximation levels. When calculating the energy of formation of complexes **I** and **II** from the NH_3 and H_2 molecules, the basis set superposition error (BSSE) [18] was disregarded, because the BSSE is not a physical effect; the question of whether this error should be taken into account remains debatable [19–23]. When the BSSE is taken into account [23], the thermodynamic stability of various multimolecular complexes and their bonding energies decrease substantially (for example, the inter-

Table 1. Results of CCD(full)/6-311++G(3*df*, 2*p*) calculations for structures **I–VI**, NH_3, and H_2

Structure	Symmetry	$-E_{tot}$	ZPE	λ	ΔE	ΔE_{ZPE}	ΔH	ΔG	$\omega_1/i\omega_1$
I	C_{3v}	57.656879	0.047035	0	0	0	0	0	62(*e*)
II	C_{3v}	57.656048	0.045896	0	0.52	–0.19	0.33	–1.86	37(*e*)
III	C_{3v}	57.648571	0.045240	1	5.21	4.09	4.22	3.72	*i*839
IV	D_{3h}	57.471557	0.046704	1	116.29	116.08	114.31	119.46	*i*1253
V	C_{3v}	57.543056	0.050487	2	71.42	73.59	71.68	76.57	*i*465(*e*)
VI	C_{2v}	57.546647	0.049632	1	69.17	70.80	69.28	73.15	*i*936
NH_3	C_{3v}	56.486124	0.034943	0	0	0	0	0	1055
NH_3	D_{3h}	56.477224	0.033524	1	5.58	4.07	4.05	4.52	*i*840
H_2	$D_{\infty h}$	1.1707166	0.010080	0	–	–	–	–	4425

Note: E_{tot} (au) is the total energy (1 au = 627.5095 kcal/mol); ZPE (au) is the zero-point energy in the harmonic approximation; λ is number of negative Hessian eigenvalues; ΔE (kcal/mol) is the energy difference; ΔE_{ZPE} (kcal/mol) is the energy difference including the zero-point energy in the harmonic approximation; ΔH and ΔG (kcal/mol) are the enthalpy and Gibbs energy differences at standard conditions ($p = 1$ atm, $T = 298.1$ K); and ω_1 (or $i\omega_1$) is the lowest (or imaginary) frequency of harmonic vibrations.

action energy for the alanine dimer was found to be –19.7 kcal/mol, whereas calculations with the BSSE included yielded +14.4 kcal/mol [23]). All the calculations were performed for the gas phase.

The tunnel splittings of the lower vibrational levels corresponding to the pyramidal inversion of the ammonia molecule in the $NH_3\cdots H_2$ complex in the two-well potential, whose minima, correspond to the complexes **I** and **II**, were calculated in the one-dimensional approximation by using the Schrödinger equation with the Hamiltonian

$$H = -\frac{1}{2}\frac{d^2}{ds^2} + V(s),$$

where $V(s)$ is the adiabatic potential of the inversion, and s is the distance along the intrinsic reaction coordinate (IRC) [10] expressed in atomic units. For comparison, the tunnel splittings for an isolated ammonia molecule were determined in the same approximation. The potential $V(s)$ determined from quantum-chemical calculations was approximated by a piecewise linear function with segments of length $\Delta s \approx 0.4$ au.

RESULTS AND DISCUSSION

Stationary Points on the PES of the $NH_3\cdots H_2$ Complex

Ab initio calculations showed that the PES of the NH_5 system has at least six stationary points corresponding to structures **I–VI**. The structures of the radicals and the structures formed by the dissociation of the ammonia molecule were not considered. Calculations show that structures **I** and **II** correspond to minima ($\lambda = 0$); structures **III**, **IV**, and **VI**, correspond to saddle points ($\lambda = 1$); and structure **V**, corresponds to a two-dimensional hill ($\lambda = 2$). The total energies, energy differences, and zero-point energies (ZPE) calculated in the harmonic approximation for structures **I–VI** and the isolated ammonia and hydrogen molecules are listed in

Table 1. The optimized geometric parameters of isomers **I–VI** and the NH_3 and H_2 molecules are presented in Fig. 1 and Table 2.

The results for NH_3 and H_2 are in good agreement with the experimental data reported in [24]. According to the calculation results, dipole complex **I** has symmetry C_{3v} and an $N\cdots H$ distance somewhat longer than the sum of Van der Waals radii of the nitrogen and hydrogen atoms (2.66 Å) [25] and shorter than the intermolecular distance in the $H_2\cdots N_2$ complex (3.40 Å) [26]. The energy of formation of complex **I** is negative though very small (–0.024 kcal/mol), whereas the energy of formation of **II** is positive (0.497 kcal/mol). Consequently, complex **II** is unstable and decomposes to yield $NH_3 + H_2$.

To our knowledge, complex **I** has not been observed experimentally; therefore, we can correlate the calculated energy of formation of this complex only with the experimental (0.0692 ± 0.0035 kcal/mol) and theoretical (0.103 kcal/mol) values of the energy of formation of the $H_2\cdots N_2$ dimeric complex [26]. Note that the allowance for ZPE markedly decreases the energies of formation of complexes **I** (0.611 kcal/mol) and **II**

Table 2. Measured and ab initio calculated geometric parameters of the NH_3 and H_2 molecules

Method	NH_3 $r(N-H)$, Å	NH_3 $\varphi(H-N-H)$, deg	H_2 $r(H-H)$, Å
RHF	1.001	107.6	0.733
RMP2/DZ	1.012	106.1	0.734
RMP2/TZ	1.013	107.3	0.738
CCD	1.013	107.1	0.743
Experiment [24]	1.0156	107.28	0.74142

Note: r is the bond length, and φ is the valence angle; CCD denotes CCD(full)/6-311++G(3*df*, 2*p*).
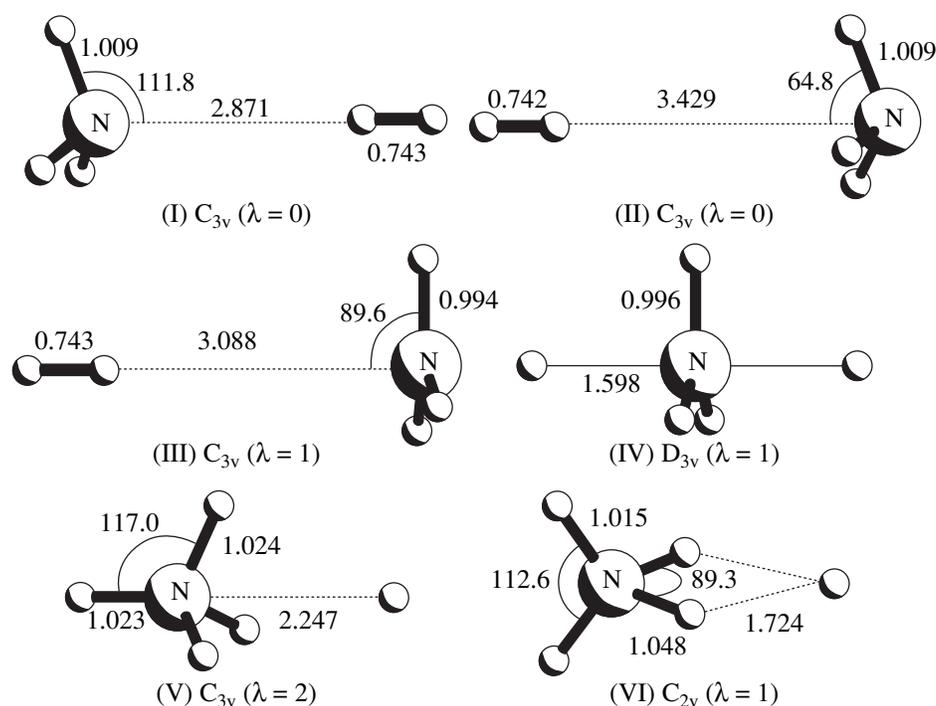
Fig. 1. Geometrical parameters of structures **I**–**VI** obtained by ab initio calculations. The bond lengths and valence angles are expressed in angstroms and degrees, respectively.

(0.418 kcal/mol); in this case, structures **I** and **II** become instable and decompose to $NH_3 + H_2$. At the same time, the presence of sufficiently pronounced minima in the PES that correspond to complexes **I** and **II** suggests that the weakly bonded complex $NH_3 \cdots H_2$ can be fixed in the hydrogen matrix at a low temperature. The lengths of the valence bonds and angles in the NH_3 and H_2 moieties of complexes **I** and **II** differ only

slightly from the respective values in the isolated molecules.

Pyramidal Inversion of the Ammonia Molecule

The inversion of the ammonia molecule in the $NH_3 \cdots H_2$ complex yields transition state **III**, which corresponds to a saddle point ($\lambda = 1$) in the PES of NH_5 with an energy barrier of 5.21 kcal/mol. This barrier is slightly lower than the calculated barrier for the inversion of an isolated ammonia molecule (5.58 kcal/mol) [24]. It is interesting to compare the tunnel splitting of the vibrational levels corresponding to the inversion of the ammonia molecule in complex **I** and the tunnel splitting for the inversion of an isolated ammonia molecule. The inverse-state vibrational levels calculated in the one-dimensional approximation are presented in Fig. 2 and listed in Table 3. In Fig. 2, curve *1* represents the potential energy curve for the **I** $\rightleftharpoons$ **III** $\rightleftharpoons$ **II** inversion while curve *2* shows the potential energy curve for the inversion of an isolated ammonia molecule. The five lower vibrational levels in the two-well potential for an isolated ammonia molecule (on the left-hand side) correspond to the six levels of the **I** $\rightleftharpoons$ **III** $\rightleftharpoons$ **II** inversion (on the right-hand side).

The calculated energies of the vibrational levels for the inversion of the ammonia molecule in the $NH_3 \cdots H_2$ complex and in the isolated ammonia molecule, as well as the measured energies of the vibrational levels for the inversion of the ammonia molecule from [24], are
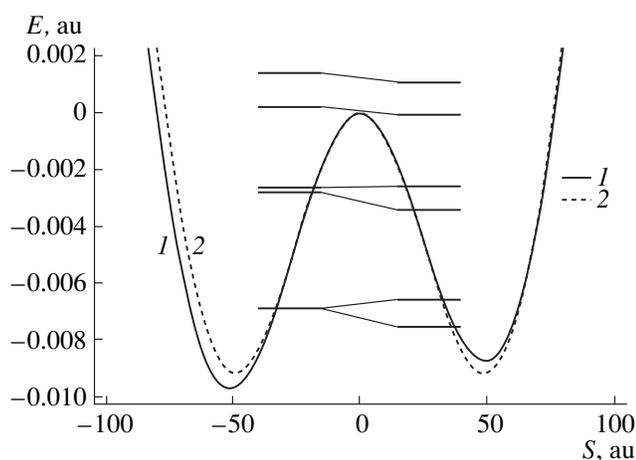
Fig. 2. Tunnel splitting of the vibrational levels corresponding to the inversion of the isolated ammonia molecule (on the left-hand side) and the NH_3 molecule in the $NH_3 \cdots H_2$ complex (on the right-hand side): (*1*) the inversion potential of the ammonia molecule in the $NH_3 \cdots H_2$ complex, and (*2*) the inversion potential of the isolated ammonia molecule.

listed in Table 3. The spacing between the two lower levels for the $NH_3 \cdots H_2$ complex is much larger than that for the ammonia molecule, whereas the other levels differ only slightly. The transition between the two lower inversion levels for an isolated ammonia molecule lies in the microwave region [27], whereas, for the $NH_3 \cdots H_2$ complex, this transition can be observed in the IR region.

Transformation of the PES along the Reaction Coordinate

Bipyramidal structure **IV** of symmetry D_{3h} corresponds to a saddle point ($\lambda = 1$) and represents the true transition state for the S_N2 reaction at the nitrogen atom. The reaction coordinate (the line of steepest descent) comes out from **IV** along the direction tangential to the transition vector and comes to another stationary point with $\lambda = 2$, structure **V**. The point symmetry group C_{3v} remains invariant along the reaction coordinate. One of the two lines of steepest descent coming out from **V** in the directions tangential to the two Hessian eigenvectors corresponding to the doubly degenerate negative eigenvalue (the e symmetry) [27, p. 241] comes to saddle point **VI** ($\lambda = 1$), while the other finishes at minimum **I** ($\lambda = 0$).

The unusual position of the second-order saddle point in the reaction coordinate can be explained on the basis of Fig. 3, which shows the results of MP2/6-31G** calculations of the variations of the vibrational modes corresponding to the Hessian eigenvalues, which are negative at one of the two saddle points under consideration. For structure **IV**, the mode s corresponding to the asymmetrical stretching along the third-order axis (the "umbrella handle") is the decomposition mode. The mode b, which corresponds to the deviation from the C_3 axis has two degenerate positive eigenvalues. The **IV** ⟶ **V** steepest descent corresponds to the asymmetrical stretching–contraction of the "umbrella handle." For the **IV** ⟶ **V** transition, the line of steepest descent in the slope of the PES has a bifurcation point (a valley-ridge inflection (VRI) point) at which the b modes become negative. In the reaction coordinate below this point, the negative stretching mode s becomes positive. At the end point (state **V**), the two negative Hessian eigenvalues correspond to two modes of deviations from the C_3 axis [16]. Figure 4 shows a schematic view of the PES along the reaction coordinate at the section of the two-dimensional mode s. This unusual topology of the PES (observed for the first time) leads to the following important conclusions:

(1) There is no limitation on the distribution of stationary points of different types over the PES. Up to now, it has been believed that such limitations are imposed by the Morse ratios. However, the Morse ratios are applicable only to distributions of nondegenerate stationary points in bounded regions of ($3N$–6)-dimensional PESs. The necessity of excluding all degenerate stationary

Table 3. Vibrational levels corresponding to the inversion of the ammonia molecule in the $NH_3 \dots H_2$ complex and the isolated NH_3 molecule (cm^{-1})

n	$NH_3 \dots H_2$ Calculation	NH_3 Calculation	NH_3 Experiment [24]
0	0	0	0
1	202.91	1.02	0.79
2	907.24	903.67	932.43
3	1089.09	938.59	968.12
4	1638.25	1568.48	1598.47
5	1898.23	1825.47	1882.18
6	2364.02	2313.31	2384.17
7	2819.79	2785.81	2895.61

Note: n is the quantum number equal to the number of nodes in the wave function.

points and poles from consideration makes the Morse ratios unsuitable for practical purposes.

(2) It is impossible to introduce rigid rules for symmetry elements (point symmetry groups) that would hold in passing from one minimum (the reactant) through the transition state structure to the other minimum (the product). The conventional rules of symmetry conservation are based on the assumption that the reaction coordinate, which connects the two minima (the reactant and product) and passes through the saddle point corresponding to the transition state, is a unique, smooth, and uniformly continuous line of steepest descent without other stationary points. Then, in accordance with the Pearson theorem [28, 29], all of the symmetry elements of the molecular structure corresponding to a nonstationary point in this line remain invariant along the reaction coordinate. In this case, a point symmetry group that remains invariant along the
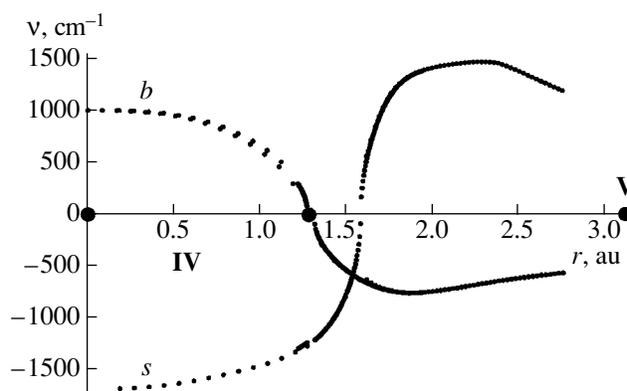
Fig. 3. Behavior of the s and b modes of structures **IV** and **V** along the steepest-descent line from **IV** to **V**; r is the distance along the reaction coordinate expressed in atomic units, and ν is the frequency.
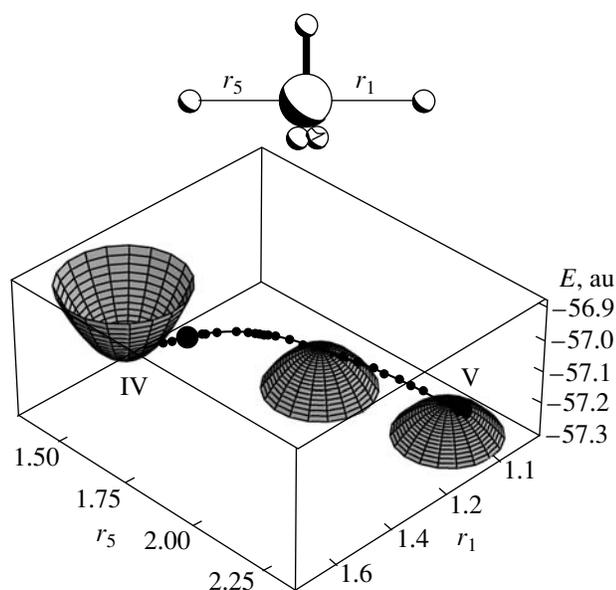
Fig. 4. A schematic two-dimensional representation of the PES in terms of the bending mode *s* along the of steepest-descent line from **IV** to **V**. The reaction coordinate is represented in terms of the r_1 and r_5 coordinates expressed in angstroms.

reaction coordinate is a subgroup of point symmetry groups of the reactant, transition state structure, and product. However, in the presence of another stationary point with $\lambda \geq 1$, at which the reaction coordinate changes its direction, the system passes from one gradient line onto another gradient line with invariant symmetry elements that can be unrelated to those of the first line. When the reaction coordinate has a second-order saddle point, as in our case, this point can be the origin of an infinite number of lines of descent with all kinds of invariant symmetry elements, i.e., with sets of symmetry elements unrelated to the symmetry of the reactant.

Thus, the ab initio calculations performed show that the reaction coordinate can have a second-order saddle point, and, consequently, there are no limitations on the distribution of stationary points of different types over the reaction coordinate. This means that it is impossible to introduce rigid rules of conservation of point symmetry throughout the reaction coordinate. The weak dipole interaction between the ammonia and hydrogen molecules stabilizes the linear C_{3v} configuration of the $NH_3 \cdots H_2$ complex.

ACKNOWLEDGMENTS

REFERENCES

1. G. A. Jeffrey and W. Saenger, *Hydrogen Bonding in Biological Structures* (Springer, Berlin, 1991).
2. C. L. Perrin and J. B. Nielsen, Annu. Rev. Phys. Chem. **48**, 511 (1997).
3. P. Hobza, H. L. Selzle, and E. W. Schlag, Chem. Rev. **94**, 1767 (1994).
4. S. Scheiner, Acc. Chem. Res. **27**, 402 (1994).
5. M. S. Gordon and J. H. Jensen, Acc. Chem. Res. **29**, 536 (1996).
6. *Principles of Molecular Recognition*, Ed. by A. D. Buckingham, A. C. Legon, and S. M. Roberts (Blackie Academic and Professional, London, 1993), pp. 16–42.
7. J. Sadlej, S. M. Cybulski, and M. M. Szczesniak, J. Phys. Chem. **100**, 10875 (1996).
8. R. M. Minyaev, Int. J. Quantum Chem. **4**, 105 (1994).
9. R. M. Minyaev and D. J. Wales, J. Chem. Soc., Faraday Trans. **90**, 1831 (1994).
10. K. Fukui, Acc. Chem. Res. **14**, 363 (1981).
11. W. Quapp and D. Heidrich, Theor. Chim. Acta **66**, 245 (1984).
12. R. M. Minyaev, Usp. Khim. **63**, 883 (1994).
13. D. A. Hrovat and W. T. Borden, J. Am. Chem. Soc. **114**, 5879 (1992).
14. W. Quapp, J. Theor. Comput. Chem. (in press).
15. L. J. Shaad and J. Hu, J. Am. Chem. Soc. **120**, 1571 (1998).
16. D. Heidrich and W. Quapp, Theor. Chim. Acta **70**, 89 (1986).
17. M. J. Frisch, G. W. Trucks, H. B. Schlegel, *et al.*, Gaussian 98, Revision A9 (Gaussian, Pittsburgh PA, 1998).
18. R. Cammi, R. Bonaccorsi, and J. Tomasi, Theor. Chim. Acta **68**, 271 (1985).
19. F. B. V. Duijnevelt, J. G. C. M. V. Duijneveld-Van De Rijdt, and J. H. V. Lenthe, Chem. Rev. **94**, 1873 (1994).
20. F. F. Muguet and G. W. Robinson, J. Chem. Phys. **102**, 3643 (1995).
21. G. Lendvay and I. Maer, Chem. Phys. Lett. **297**, 365 (1998).
22. S. Simon, M. Duran, and J. J. Dannenberg, J. Chem. Phys. **105**, 11024 (1997) (see references therein).
23. D. B. Cook, T. L. Sordo, and J. A. Sordo, J. Chem. Soc., Chem. Commun., 185 (1990).
24. V. Spirko, J. Mol. Spectrosc. **101**, 30 (1983).
25. Yu. V. Zefirov and P. M. Zorkii, Russ. Chem. Rev. **64**, 446 (1995).
26. P. Hobza and R. Zahradnik, Chem. Rev. **88**, 871 (1988).
27. P. F. Bernath, *Spectra of Atoms and Molecules* (Oxford Univ. Press, New York, 1995).
28. R. Pearson, Theor. Chim. Acta **16**, 107 (1970).
29. R. Pearson, *Symmetry Rules for Chemical Reactions*, (Wiley, New York, 1976; Mir, Moscow, 1979).